TARGET DETECTION WITH TEXTURE FEATURE CODING METHOD AND SUPPORT VECTOR MACHINES

J. Liang, X. Zhao, R. Xu, and C. Kwan
Intelligent Automation, Inc.
7519 Standish Place, Suite 200
Rockville, MD 20855, USA
ckwan@i-a-i.com

C-I Chang
U. Maryland at Baltimore County
Department of Computer Science and Electrical Engineering
Baltimore, MD 21250

Abstract

A texture analysis approach of using an improved texture feature coding method (TFCM) and the Support Vector Machines (SVM) for target detection is presented in this paper. Preliminary test on mammogram showed over 88% of normal mammograms and 85% of abnormal mammograms were correctly identified. Automatic target detection with a Cascade-Sliding-Window (CSW) technique is also discussed.

1. Introduction

Automatic Target Recognition has many applications. Detection of land mines, mass graves, weapon concealment, etc. is hard by visual inspection of images collected from various airborne sensors. In some cases, it was observed that ground breaking will cause soil texture change and hence observation of texture difference from surroundings may indicate the presence of land mine, mass graves, weapon concealment, etc [1]. In medical practices, it is an objective that an anomaly be correctly identified from a mammogram without false alarms. Many researches have been conducted in this perspective by using imaging texture analysis [2].

TFCM is a new texture analysis scheme which transforms an original image into a text feature image whose pixels represent texture feature numbers. This coding scheme has several remarkable advantages, including more accurate representation of texture information, more computationally efficient, better capture of texture information by incorporating higher-order gradient information, etc [3]. SVM is a learning and classification tool originated from modern statistical learning theory [4]. It is a kernel based learning algorithm and relies on the borderline training samples to define the separation hyperplane. Its performance is better than most learning systems for a wide range of applications including automatic target recognition, image detection, and document classification.

This paper focuses on the investigation of the potential benefit of using TFCM and SVM for target detection. Section 2-4 summarizes the TFCM approach, the feature descriptor, and the SVM classification method. Experimental results using mammograms are reported in Section 5. Finally, concluding remarks are given in Section 6.

2. Texture Feature Coding Method

The concept of the TFCM method is derived from the gray-level co-occurrence matrix [5] and texture spectrum method [6]. It was first developed by Horng [3]. Some of the major points of this algorithm are briefly described here.

Figure 1(a) shows a 3x3 window mask over a pixel, in which there are eight orientations, 0^o, 45^o, 90^o, 135^o, 180^o, 225^o, 270^o, 315^o. Figure 1(b) shows the 4-neighbor connectivity of the pixel X by four pixels labeled by 1, 3, 5, 7 referred to as the first-order neighboring pixels. The additional four pixels labeled by 2, 4, 6, 8 located along two diagonal lines are referred to as second-order neighboring pixels as shown in Fig. 1(c).

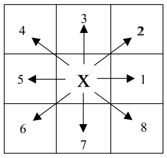

(a) 8 orientations

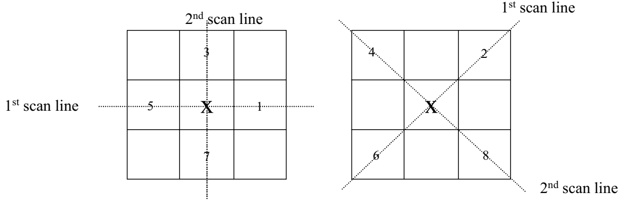

(b) first-order 4-neighbor connectivity (c) second-order 4-neighbor connectivity

Fig. 1 First-order and second-order 4-neighbor connectivity

TFCM method considers three consecutive pixels along these specific directions, and calculates gradient changes in gray levels among these three pixels [3]. Denote three consecutive pixels by their spatial coordinates at *a*, *b*, *c* and associated gray levels by $I(a)$, $I(b)$ and $I(c)$ respectively, and let Δ be a desired gray level tolerance. There are four types of successive gradient changes in gray level with their corresponding graphic descriptions given in Fig. 2.

$$
\begin{array}{lll}
\text{(i)} & |I(a)-I(b)|\le\Delta,\ |I(b)-I(c)|\le\Delta & \\
\text{(ii)} & |I(a)-I(b)|\le\Delta,\ |I(b)-I(c)|>\Delta & \text{or} \\
 & |I(a)-I(b)|>\Delta,\ |I(b)-I(c)|\le\Delta & (1) \\
\text{(iii)} & I(a)-I(b)>\Delta,\ I(b)-I(c)>\Delta & \text{or} \\
 & I(b)-I(a)>\Delta,\ I(c)-I(b)>\Delta & \\
\text{(iv)} & I(a)-I(b)>\Delta,\ I(c)-I(b)>\Delta & \text{or} \\
 & I(b)-I(a)>\Delta,\ I(b)-I(c)>\Delta &
\end{array}
$$

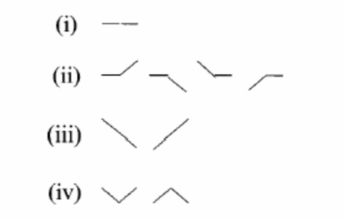

Fig. 2 Types of gray-level graphical structure variations

0-7803-8484-9/04/$20.00 ©2004 IEEE

If we introduce a pair of integers (*a*,*b*) to represent the gray-level variations of first-order and second-order connectivity, respectively, and consider the symmetry between first scan line and second line of first-order or second order connectivity, the number of each connectivity combinations can be reduced to 4(4+1)/2=10, as shown in Table 1.

Table 1 Combination coding of the gray-level variations

First scan line

Second scan line

	(i)	(ii)	(iii)	(iv)
(i)	1	2	3	4
(ii)	2	5	6	7
(iii)	3	6	8	9
(iv)	4	7	9	10

Furthermore, if we ignore the difference between the first order and second order connectivity, we can define the text feature number $TFN_{\Delta}(x,y)$, of the pixel at location (*x*,*y*) according to Table 2.

Table 2 Texture Feature Number Generation Table

a b	1	2	3	4	5	6	7	8	9	10
1	0	1	2	3	4	5	6	7	8	9
2	1	10	11	12	13	14	15	16	17	18
3	2	11	19	20	21	22	23	24	25	26
4	3	12	20	27	28	29	30	31	32	33
5	4	13	21	28	34	35	36	37	38	39
6	5	14	22	29	35	40	41	42	43	44
7	6	15	23	30	36	41	45	46	47	48
8	7	16	24	31	37	42	46	49	50	51
9	8	17	25	32	38	43	47	50	52	53
10	9	18	26	33	39	44	48	51	53	54

It is worth mentioning that this coding scheme has three unique properties. First, the $TFN_{\Delta}(x,y)$ is quasi-rotation-invariant because the symmetry is considered during coding. Second, since $TFN_{\Delta}(x,y)$ only takes a value ranging from 0 to 54, the calculation of a TFCM based co-occurrence matrix of an image and some of its corresponding TFCM features will take less time. Third, the code value at a given pixel represents the coarseness in its neighborhood. The higher the code value is, the more gray-level variations its corresponding pixel possesses. All aforementioned properties are very important as they capture essence of the texture around a specific pixel.

After a TFN feature image is obtained by TFCM, there are two measures, i.e., TFN histogram and TFCM-based Co-occurrence matrix, to characterize its statistics. A TFN histogram is defined as

$$p_{TFN,\Delta}(n)=\frac{N_{TFN,\Delta}(n)}{\sum_{n=0}^{54}N_{TFN,\Delta}(n)} \tag{2}$$

where $N_{TFN,\Delta}(n)$ is the total number of $TFN_{\Delta}(x,y)$ in the image taking value *n*, and Δ is the gray-level variation tolerance given in (1). The TFN based co-occurrence matrix, which is a probability distribution of transitions between any pair of arbitrary two TFNs, can be defined as

$$p_{\Delta}(i,j\,|\,d,\theta)=\frac{N_{\Delta,d,\theta}(i,j)}{\sum_{l,k}N_{\Delta,d,\theta}(l,k)} \tag{3}$$

where $N_{\Delta,d,\theta}(i,j)$ is the number of pairs of two pixels at spatial locations (*x*,*y*) and (*w*,*z*) satisfying TFN code level *I*(*x*,*y*) = *i*, *I*(*w*,*z*) =*j* and *d*-pixel apart along angular rotation θ. $\sum_{l,k}N_{\Delta,d,\theta}(l,k)$ is the total number of TFN transitions.

3. Statistical Texture Feature Descriptors

In order to capture the essence of texture information of an image, a set of texture feature descriptors was developed to represent the kernel texture information of the image. Here we introduce eleven descriptors. Some of them are well known [3][7], and some are specially designed for the mammogram data.

The first two feature descriptors are derived from the TFN histogram of an image.

1. Mean convergence

$$MC=\sum_{n=0}^{54}\frac{\left|n\cdot p_{\Delta}(n)-\mu_{\Delta}\right|}{\sigma_{\Delta}}. \tag{4}$$

2. Code variance

$$Var=\sum_{n=0}^{54}\left(n-\mu_{\Delta}\right)^{2}\cdot p_{\Delta}(n) \tag{5}$$

The remaining descriptors are based on the TFN co-occurrence matrix. Here we fixed $d=1$ and used the average of four matrices, corresponding to $\theta=0^{0}$, $\theta=45^{0}$, $\theta=90^{0}$ *and* $\theta=135^{0}$, respectively. That is:

$$P_{\Delta,d}=\frac{1}{4}\left(P(d=1,\theta=0^{0})+P(d=1,\theta=45^{0})+P(d=1,\theta=90^{0})+P(d=1,\theta=135^{0})\right)$$

where $P(d,\theta)$ is the TFN co-occurrence matrix with respect to d and θ .Based on $P_{\Delta d}$, we define the following features

3. Code entropy

$$CE=\sum_{i=0}^{54}\sum_{j=0}^{54}p_{\Delta,d}(i,j)\log p_{\Delta,d}(i,j) \tag{6}$$

4. Uniformity

$$UN=\sum_{i=0}^{54}\sum_{j=0}^{54}p_{\Delta,d}^{2}(i,j) \tag{7}$$

5. First-order element difference moment (FDM)

$$FDM=\sum_{i=0}^{54}\sum_{j=0}^{54}\left|i-j\right|p_{\Delta,d}(i,j) \tag{8}$$

6. Second-order element difference moment (SDM)

$$SDM=\sum_{i=0}^{54}\sum_{j=0}^{54}(i-j)^{2}p_{\Delta,d}(i,j) \tag{9}$$

7. First-order inverse element difference moment (FIDM)

$$FIDM=\sum_{i=0}^{54}\sum_{j=0}^{54}\frac{1}{1+\left|i-j\right|}p_{\Delta,d}(i,j) \tag{10}$$

8. Second-order inverse element difference moment (SIDM)

$$SIDM=\sum_{i=0}^{54}\sum_{j=0}^{54}\frac{1}{1+(i-j)^{2}}p_{\Delta,d}(i,j) \tag{11}$$

9. Energy Distribution of Co-occurrence Matrix

The following three features are the summations of different regions of the co-occurrence matrix.

$$SB1=\sum_{i=44}^{54}\sum_{j=44}^{54}p_{\Delta,d}(i,j) \tag{12}$$

$$SB2=\sum_{i=34}^{54}\sum_{j=34}^{54}p_{\Delta,d}(i,j)-SB1 \tag{13}$$

$$SB3=\sum_{i=14}^{54}\sum_{j=14}^{54}p_{\Delta,d}(i,j)-SB1-SB2 \tag{14}$$

Their summation regions are depicted in Fig. 3.

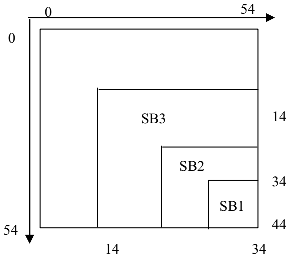

Fig. 3. Summation regions of different subband probabilities.

As a result, each image in the database is represented by an 11 x 1 feature vector. Since some of the features usually have large magnitudes and others have small magnitudes, we scale different feature elements such that each feature contributes roughly equally to the SVM. For the mammogram data, the scaling factors were, scale = [1, 1, 20, 1E4, 1, 10, 100, 100, 100, 100, 100].

4. Support Vector Machines and Classification Steps

According to references [8-10], the key elements in the implementation of SVM are the mathematical programming and kernel functions. SVM parameters are found by solving a quadratic programming problem with linear equality and inequality constraints; rather than by solving a non-convex, unconstrained optimization problem. The flexibility of kernel functions allows the SVM to search a wide variety of hypothesis spaces. The geometrical interpretation of support vector classification (SVC) is that the algorithm searches for the optimal separating surface, i.e. the hyperplane that is, in a sense, equidistant from the two classes. A simple example of 2-D data classification with three different classes using SVM is shown in Fig. 4, where the optimal boundaries are found between each pair of classes.

Fig. 4 SVM classification results of three classes

In our study, a Matlab toolbox was developed to perform image texture analysis and classification. The TFCM-SVM training and testing procedures are brief summarized.

1. Prepare *N* training images with known ground truth. Associate each image with an integer class label, for example, 0, 1, 2,…*N*, as required by the OSU-SVM.
2. Perform TFCM on each image to obtain a feature image with its element being TFN numbers.
3. Calculate a TFN histogram for each feature image.
4. Calculate a TFCM co-occurrence matrix for the same feature image
5. Calculate the 11 texture feature descriptors using Eqs. (9) to (17) to represent the image being processed
6. Form all the image feature vectors into a 11x*N* matrix, regarded as the input matrix. Align their class labels to a 1x*N* row output vector.
7. Use the input and output pair to train the OSU-SVM. The result is stored in a set of vectors and matrices.

In the test stage, the first six steps still applicable to a test image, while in the last step, the trained support vector machine outputs a label vector for the test image.

5. Mammogram Inspection Using TFCM-SVM

Our first case study is focused on mammogram inspection using the TFCM-SVM. The database is the MiniMammographic Database provided by the Mammographic Image Analysis Society (MIAS). In our simulation study, 69 normal mammogram images and 55 abnormal images containing different abnormalities were segmented from the database. The abnormal regions belong to 5 abnormal categories:

- 13 architectural distortions (ARCH),
- 10 asymmetry tissues (ASYM),
- 12 circumscribed masses (CRIC),
- 11 speculate masses (SPEC),
- 9 other/ill-defined masses (MISC).

In the simulations, we run the TFCM method on the above five categories of well-defined/circumscribed masses, speculated masses, architectural distortion (ad), asymmetry, and other/ill-defined masses and some sample images are shown in Fig. 5.

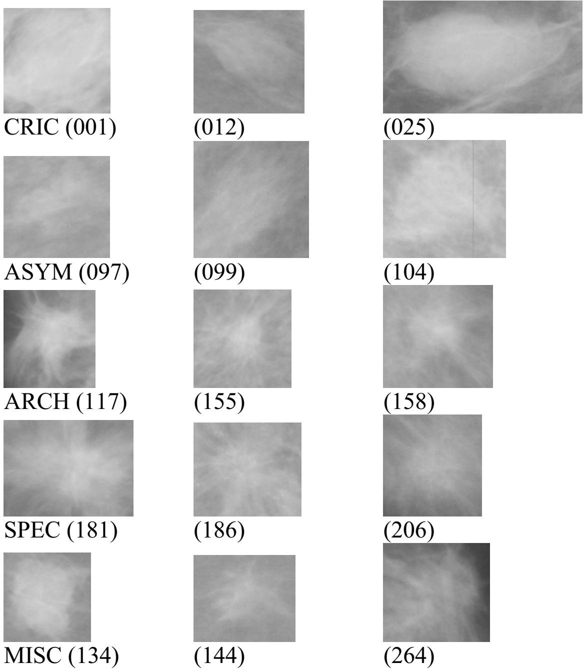

CRIC (001) (012) (025)

ASYM (097) (099) (104)

ARCH (117) (155) (158)

SPEC (181) (186) (206)

MISC (134) (144) (264)

Fig. 5 Five categories of abnormal images, each begins with their label and image number in the library.

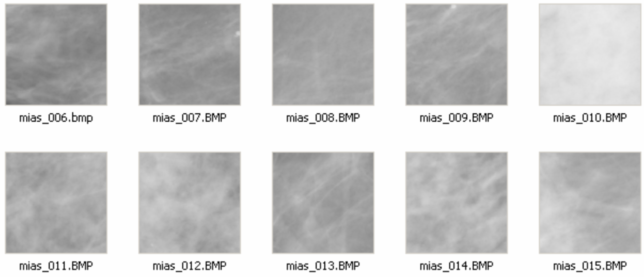

Fig. 6 Normal training images

All normal images are 128x128 in size whereas the image size for the abnormal images varies as the area of the abnormal region differs from one case to another. Figure 6 shows some of the normal training images.

After obtaining the features of each image in the database, we use the SVM to perform the classification. The performance of the SVM is affected by two parameters, namely the kernel parameter γ and the regularization parameter C.

Table 3 Performance of TFCM-SVM with $C = 100$

γ	Training Error Rate	Correct Decision Rate of Normal Data	Correct Decision Rate of Abnormal Data	Overall Correct Decision Rate
$1E-3$	6 %	47/59=80%	39/55=71%	86/114=75%
$1E-4$	**11 %**	**53/59=90%**	**44/55=80%**	**97/114=85%**
$1E-5$	16%	53/59=90%	39/55=71%	92/114=81%

Table 4 Performance of TFCM-SVM with $\gamma = 1E-4$

C	Training Error Rate	Correct Decision Rate of Normal Data	Correct Decision Rate of Abnormal Data	Overall Correct Decision Rate
1E3	7%	52/59=88%	45/55=82%	97/114=85%
1E4	**3%**	**52/59=88%**	**47/55=85%**	**99/114=87%**
1E5	0%	52/59=88%	44/55=80%	96/114=84%

In Table 3, we fix C as 100, and show the results with $\gamma = 1E-3$, $\gamma = 1E-4$, and $\gamma = 1E-5$, respectively. The cross validation method was used in the training and test. It can be observed that the best classification result is obtained with $\gamma = 1E-4$. In this case, the algorithm yields 90% correct decision for normal data and 80% correct classification for abnormal data. The overall correct decision rate is 85%. We then fix γ as $1E-4$ and vary the value of C. The results are summarized in Table 4, which shows that the best performance if given by $C = 1E4$ and $\gamma = 1E-4$. Although the classification performance of normal data is slightly reduced, the performance for abnormal data is improved, and the overall correct classification rate increases to 87%. The effect of SVM parameters can also be clearly observed from these tables. For a given regularization parameter C, larger kernel parameter γ leads to less training errors. However, the generalization capability of the SVM to test data is reduced. But if γ becomes too small, the two classes would be too close to each other, and the performance will also degrade. In a short, there is an optimal combination of the two SVM parameters, which can be obtained during experiment through try-and-error.

In order for the program to detect and localize a target automatically, a Cascade Sliding Window (CSW) technique was developed. The key idea is to segment the whole image by a $N \times N$ pixel window and train the TFCM-SVM by both the normal region and the target region. For testing a new image, the $N \times N$ pixel window moves around the image and feeds the segmented image into the TFCM_SVM for classification. The flowchart diagram of CSW is shown in figure 7. Figure 8 shows two sampled results, where a yellow ellipsis is known as ground truth and red frames are the CSW detected targets.

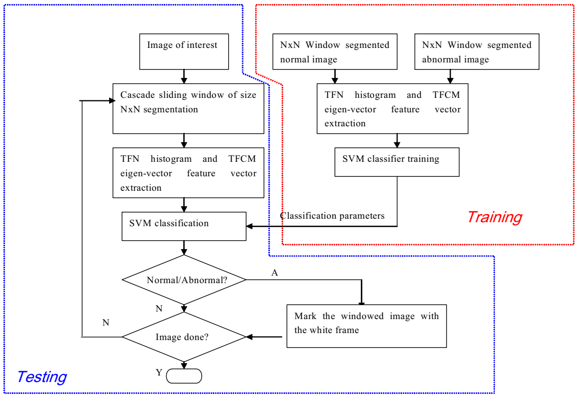

Fig. 7 Flow chart of the TFCM-SVM-CSW algorithm

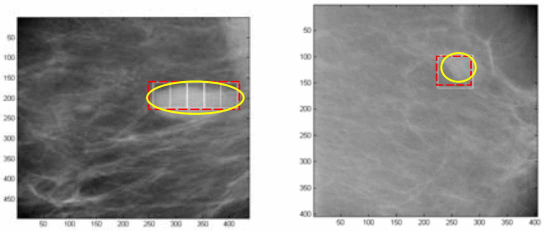

Fig. 8 Anomaly detection and localization in mammograms with CSW

6. Conclusions

A texture analysis algorithm using texture feature coding method (TFCM) and the support vector machines (SVM) for target detection is developed. Preliminary test on mammogram showed over 88% of normal mammograms and 85% of abnormal mammograms were correctly identified. Cascade-Sliding-Window (CSW) technique showed great potential for automatic target detection.

Acknowledgment

This research was supported by Navy under contract number N68335-03-C-0034

References

[1] C. Kwan et al., Phase 1 final report to the Navy, July, 2003.
[2] S. Beag and N. Kehtarnavaz, "Texture based Classification of Mass Abnormalities in Mammograms," IEEE, 2000.
[3] M. H. Horng, "Texture feature coding method for texture classification," Opt. Eng., Vol 42 (1), pp. 228-238, 2003
[4] V. Vapnik, Statistical Learning Theory. New York: Wiley 1998
[5] R.M. Harlaick, K. Shanmugam, Itshak Dinstein, "Textural features for image classification," *IEEE Trans. System, Man and Cybernetics*, vol. 3, pp. 610-621, 1973.
[6] D. C. He and L. Wang, 'Texture classification using texture spectrum," Pattern Recognition, vol. 23, pp905-910, 1990
[7] J. R. Carr and F. P. de Miranda, "The semivariogram in comparison to the co-occurrence matrix for classification of image texture," IEEE Trans. Geoscience and remote sensing, Vol. 36 (6), pp. 1945-1952, No. 1998.